Nonlinear Thouless pumping of solitons across an impurity

Xuzhen Cao,[1,2] Chunyu Jia,[3] Ying Hu,[1,2,*] and Zhaoxin Liang[3,†]

[1]*State Key Laboratory of Quantum Optics and Quantum Optics Devices, Institute of Laser Spectroscopy, Shanxi University, Taiyuan 030006, China*

[2]*Collaborative Innovation Center of Extreme Optics, Shanxi University, Taiyuan, Shanxi 030006, China*

[3]*Department of Physics, Zhejiang Normal University, Jinhua 321004, China*

(Received 5 March 2024; revised 25 June 2024; accepted 26 June 2024; published 10 July 2024)

The nonlinear Thouless pumping is an exciting frontier of topological physics. While recent works have revealed the quantized motion of solitons in Thouless pumps, the interplay between the topology, nonlinearity, and disorder remains largely unexplored. Here, we investigate the nonlinear Thouless pumping of solitons in the presence of an impurity in the context of a Bose–Einstein condensate. Using both the Gross-Pitaevskii equation and Lagrange variational approach, we analyze the interaction between a moving soliton and an impurity. Without the pump, the soliton can pass through when the impurity strength is weak; however, it can get trapped when the impurity strength increases. In contrast, we find Thouless pump soliton in Thouless pumps can transit through also for strong impurity strength, and its motion is topologically quantized. Our result explicitly showcases the robustness of topological soliton pumping against microscopic imperfections, and opens a new perspective in the information processing with solitons.

DOI: 10.1103/PhysRevA.110.013305

I. INTRODUCTION

Central to understanding quantized topological transport is the concept of Thouless pumping [1–4]. There, a quantum particle acted on by a periodic potential that varies adiabatically and periodically in time shows a quantized motion; the quantized displacement, dictated by the Chern number of the underlying band structure in the momentum-time space, is stable against disorder [4]. The experimental implementation of Thouless pumps and the observations of topologically quantized transport have been achieved in a wide variety of systems, including ultracold atoms [5–11], photonics [12–16], and spin systems [17,18]. Interestingly, these synthetic topological systems can operate even beyond the linear regime, i.e., in the presence of nonlinearities that arise from the Kerr effect in optical platforms [19–23] or the interparticle interactions in atomic setups [24–26]. At present, exploring nonlinear topological pumping has attracted significant interests and experimental efforts.

A paradigm of the nonlinear Thouless pumping concerns the topological transport of nonlinear excitations, known as solitons [27–33]. It has been shown that for weak nonlinearity, the motion of the soliton can be topologically quantized, where the quantized displacement is directly related to the topology of the underlying band structures [6–8,10–13,15,17,34,35]; whereas, the quantization breaks down in the strong nonlinearity limit [3,5,20,28,29,36–49]. More recent studies have shown that the nonlinearity can fundamentally modify the adiabatic dynamics and thus the Berry connection [33]. So far, however, exploring the interplay of nonlinear excitations, topology, and disorder remains largely unchartered territory.

In this work, we explore the soliton transport in nonlinear Thouless pumps in the presence of an impurity, based on a quasi-one-dimensional (quasi-1D) Bose-Einstein condensate (BEC). We first numerically simulate the motion of the soliton through the impurity using the Gross-Pitaevskii (GP) equation [50–52]. Further, we analytically study the interaction between the soliton and the impurity using the Lagrangian variational approach. Without the pumps, the fate of the soliton relies crucially on the effective mass of the impurity: For weak impurity strength, the soliton can easily pass through, but when the impurity strength increases, the soliton can get trapped. However, in the presence of Thouless pumps, we find the soliton can transit through the impurity, and its motion becomes topologically quantized. Such topology-enhanced soliton transport through the impurity provides insights into the interplay between nonlinearity, topology, and disorder, and explicitly elucidates the stability of the topological nonlinear pumping against local imperfections. Our result may enable possibilities in the information processing with solitons.

The paper is organized as follows. In Sec. II, we present detailed descriptions of our model system. In Sec. III, by numerically solving GP equation, we investigate the nonlinear Thouless pumping of solitons in the presence of an impurity. In Sec. IV we analytically derive the equations of motions for the soliton using Lagrangian variational approach to gain more understandings of its interaction with the soliton. Both the numerical and analytical results explicitly demonstrate the robustness of topological soliton pumping against imperfections. In Sec. VI we summarize our work.

*huying@sxu.edu.cn
†zhxliang@zjnu.edu.cn

II. MODEL SYSTEM

We consider a 3D BEC with an attractive interatomic interaction in the following trap geometry [5,6]: in the x direction, the BEC is trapped in an optical superlattice $V_{\rm OSL}(x,t)$ and an impurity potential $V_{\rm imp}$, while in the y and z directions, the BEC is tightly confined in the harmonic trap with the large trap frequency $\omega_\perp$ such that the atomic motions in these directions are affectively frozen. At the mean-field level, the considered BEC can be described by the condensate wave function $\Psi(x,y,z)=\psi(x)\phi(y,z)$ with $\phi(y,z)=1/(\sqrt{\pi}a_\perp)e^{-[y^2+z^2]/(2a_\perp^2)}$ and $a_\perp=\sqrt{\hbar/(m\omega_\perp)}$. Averaging out the transverse degrees of freedom results in an effective quasi-1D BEC described by the following GP equation [53,54], i.e.,

$$i\hbar\frac{\partial\psi}{\partial t}=-\frac{\hbar^2}{2m}\frac{\partial^2\psi}{\partial x^2}+g|\psi|^2\psi+[V_{\rm imp}(x)+V_{\rm OSL}(x,t)]\psi. \tag{1}$$

Here the m is the atomic mass, and $g=2\hbar^2a_s/(ma_\perp^2)$ is the confinement-modified coupling constant, where $a_s<0$ is the negative s-wave scattering length.

In Eq. (1), we consider the time-dependent superlattice potential $V_{\rm OSL}/E_R=-V_s\cos^2(\frac{2\pi x}{d})-V_l\cos^2(\frac{\pi x}{d}-\Omega t)$, with $E_R=\hbar^2\pi^2/(2md^2)$. It consists of a primary lattice with the spatial period $d/2$ and lattice strength V_s, and a superimposed second lattice with the period d and the strength V_l; the relative phase between the two lattices is Ωt. Such a time-dependent potential has been experimentally realized in quantum gases to implement Thouless pumps [6].

Moreover, we consider the impurity potential in Eq. (1) as $V_{\rm imp}/E_R=-V_0\delta(x)$, corresponding to an impurity centered at $x=0$ with the impurity strength V_0. Such an impurity trap has been experimentally realized using bichromatic fields [55,56], or dark-state optical potentials [57,58].

For subsequent analysis, we will rescale GP equation (1) into the dimensionless form via $x\to x/d$, $t\to 2E_Rt/\pi^2\hbar$, $\psi\to\psi\sqrt{|g|\pi^2/2E_R}$, $\gamma=V_0\pi^2/2d$, $V_{s(l)}=V_{s(l)}\pi^2/2$, and $\nu=\Omega\hbar\pi^2/2E_R$. The resulting dimensionless GP equation reads

$$i\frac{\partial}{\partial t}\psi=-\frac{1}{2}\frac{\partial^2}{\partial x^2}\psi-|\psi|^2\psi-\gamma\delta(x)\psi+V_{\rm OSL}(x,t)\psi, \tag{2}$$

with the normalization condition $\int|\psi|^2dx=N$. The dimensionless pumping potential is explicitly given by

$$V_{\rm OSL}(x,t)=-V_s\cos^2(2\pi x)-V_l\cos^2(\pi x-\nu t), \tag{3}$$

which is periodic in time with the periodicity $T=\pi/\nu$. In addition, the γ in Eq. (2) reflects the strength of the defect, and can be interpreted as the effective mass of the impurity [54].

III. SOLITONIC THOULESS PUMPING THROUGH AN IMPURITY: NUMERICAL STUDY

In this section, we numerically study the soliton motion based on the GP equation (2) under the initial excitation condition $\psi(x,0)=Ae^{-(x-x_0)^2/l^2}e^{ikx}$ [29,54], where k and x_0 denote the initial momentum and the center-of-mass position, respectively; l is the initial width of the envelope and A is the peak amplitude. The ratio $A^2/V_{\rm min}$ with $V_{\rm min}=\min(V_s,V_l)$ effectively characterizes the strength of nonlinearity in the nonlinear Thouless pump. We will specialize to the regime of sufficiently strong nonlinearity, where stable soliton forms.

Before proceeding, we briefly review three familiar cases studied before. (i) In the absence of both impurity ($\gamma=0$) and Thouless pump ($V_{\rm OSL}=0$), the quasi-1D BEC described by GP Eq. (2) is known to support solitons as the nonlinear excitations. (ii) Without impurity ($\gamma=0$), Eq. (2) with $V_{\rm OSL}\neq0$ has been used to study the nonlinear Thouless pumping of solitons such as in Ref. [29,30]. It is shown that for $A^2/V_{\rm min}$ below some critical value, i.e., in the pumped regime, the soliton undergoes topologically quantized transport, whereas for $A^2/V_{\rm min}$ above the critical value, i.e., in the trapped regime, the soliton is dynamically localized near its initial position. (iii) Equation (2) with $\gamma\neq0$ and $V_{\rm OSL}=0$ has been used to study the interaction between a moving soliton with an impurity. As shown in Refs. [53,54], the behavior of the soliton crucially depends on the impurity strength γ. Specifically, the soliton can only move through for the weak γ, but becomes to be trapped when γ increases.

In this work, we are interested in the motion of the soliton when both the pump and the impurity are present, i.e., $V_{\rm OSL}\neq0$, $\gamma\neq0$. To this end, henceforth we focus on the $A^2/V_{\rm min}$ in the pumped regime where solitons undergo topological transport in the defect-free case. We numerically solve the GP Eq. (2) by the split-step fast Fourier algorithm [59]; see Appendix A for technical details. In the numerical simulation, we approximate the δ potential by a sufficiently narrow Gaussian function according to the identity $-\gamma\delta(x)=-\lim_{\sigma\to0}\frac{\gamma}{\sqrt{2\pi}\sigma}e^{-x^2/(2\sigma^2)}$. For concreteness, we assume a pump with $V_s=V_l=25$, whose lowest band of the underlying band structure has the Chern number $C=1$ [4]. (We refer to Appendix B for detailed calculations of the Chern numbers of the underlying band structures associated with the linear Thouless pump.) In addition, we choose the initial soliton width $l<0.5$ (i.e., smaller than the half spatial periodicity), so that the soliton state mainly occupies the lowest band when projecting onto the underlying linear Bloch states. Finally, the initial soliton momentum and the pump rate are chosen as $k=0.1$ and $\nu=0.1$, respectively, to ensure the adiabatic condition required by Thouless pump. Our numerical calculations reproduce the known results described earlier in (i)–(iii). The soliton motion under different parameters will be shown in Sec. V.

Our numerical results are shown in Figs. 1(a) and 1(b) for weak γ and in Figs. 2(a) and 2(b) for large γ, respectively, where we compare the soliton behavior in the absence and presence of the topological pump. Consider first the regime of weak impurity [Fig. 1(a)] without the pump. We see that the soliton directly tunnels through the weak impurity potential centered at $x=0$, where the collision within the impurity only causes a small deviation of the soliton from its original path. In the presence of the topological pump with $V_s=V_l=25$, as shown in Fig. 1(b), the soliton not only transmits through the impurity, but also the solitonic displacement becomes quantized to the underlying Chern number of the pump, despite the presence of the impurity.

In comparison, Figs. 2(a) and 2(b) illustrate the soliton motion for large impurity mass. Without the pump, as

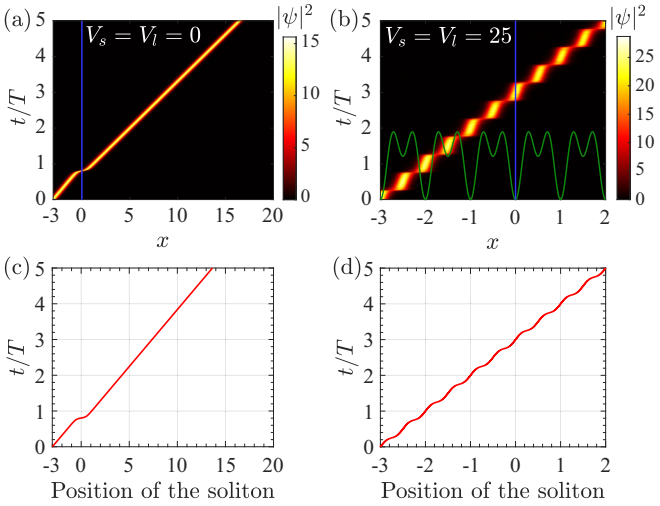

FIG. 1. Soliton transport for weak impurity strength, without and with nonlinear Thouless pumps. In (a) and (c), the pump is absent, where $V_s = V_l = 0$. In (b) and (d), the pump is present, with $V_s = V_l = 25$ and the periodicity T. In (a) and (b), the solitonic motion in space (x) and time (t/T) is simulated via the numerical solutions of the dimensionless GP Eq. (2). The impurity is numerically modeled as $-\gamma\delta(x) \approx -\frac{\gamma}{\sqrt{2\pi}\sigma}\exp(-x^2/(2\sigma^2))$, with $\gamma = 0.1$ and $\sigma = 0.002$. and the initial state $\psi(x,0) = Ae^{-(x-x_0)^2/l^2}e^{ikx}$, where $x_0 = -3$, $l = 0.4$, $k = 0.1$, $v = 0.1$, and $A^2 = 15$. The color bar denotes the magnitude of $|\psi|^2$. The blue line in (a) denotes the center of the impurity potential. The green line in (b) denotes the pumping potential at $t = 0$. (c) and (d) present the results for the center-of-mass position of the soliton based on the Euler-Lagrange Eqs. (8)–(13) with scaled parameters $\tilde{\gamma} = \gamma/A = 0.026$, and $z(0)/A = -3$, $\eta(0) = 1$, $\kappa(0) = 0.0258$, $\alpha(0) = \beta(0) = a(0) = 0$.

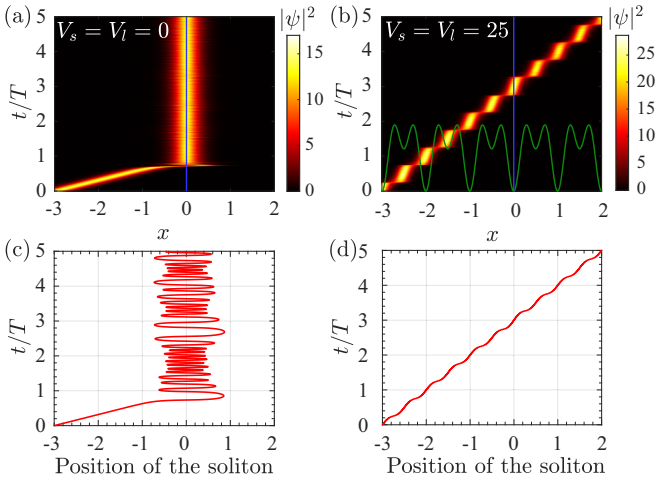

FIG. 2. Soliton transport for strong impurity strength, without and with nonlinear Thouless pumps. In (a) and (c), the pump is absent, where $V_s = V_l = 0$. In (b) and (d), the pump is present, with $V_s = V_l = 25$. In (a) and (b), the solitonic motion is simulated via the numerical solutions of the dimensionless GP equation (2) where the impurity is approximated by $-\gamma\delta(x) \approx -\frac{\gamma}{\sqrt{2\pi}\sigma}\exp[-x^2/(2\sigma^2)]$ with $\gamma = 0.53$ and $\sigma = 0.002$. The initial condition is $\psi(x,0) = Ae^{-(x-x_0)^2/l^2}e^{ikx}$, where $x_0 = -3$, $l = 0.4$, $k = 0.1$, $v = 0.1$, and $A^2 = 15$. (c) and (d) present the results for the center-of-mass position of the soliton based on the Euler-Lagrange equation Eqs. (8)–(13) with scaled parameters $\tilde{\gamma} = 0.137$ and $z(0)/A = -3$, $\eta(0) = 1$, $\kappa(0) = 0.0258$, $\alpha(0) = \beta(0) = a(0) = 0$.

illustrated in Fig. 2(a), we see that the soliton gets trapped in the impurity potential, as opposed to the case of weak impurity in Fig. 1(a). Interestingly, after applying Thouless pump with $V_s = V_l = 25$ in Eq. (3), the soliton is able to pass through the impurity instead of being localized by it [see Fig. 2(b)]. Moreover, the solitonic displacement in a period becomes quantized to unity. This phenomena contrasts strongly with the pump-free counterpart, and showcases the stability of the topological nonlinear pumping against the static disorder.

IV. SOLITONIC THOULESS PUMPING THROUGH AN IMPURITY: VARIATIONAL APPROACH

To further establish our results and gain understandings how the interaction between the soliton and the impurity is affected by the Thouless pump, in this section we develop an analytical study of the soliton motion using the Lagrangian variational approach.

We consider the renormalized wave function $\psi(x,t) = A\phi(X,\tau)e^{i(V_s+V_l)t/2}$ with the new variables $\tau = A^2t$ and $X = Ax$ [29,30], and recast Eq. (2) into the following form:

$$i\phi_\tau = -\tfrac{1}{2}\phi_{XX} - |\phi|^2\phi - \tilde{\gamma}\delta(X)\phi + \tilde{V}_{\rm OSL}(X,\tau)\phi. \quad (4)$$

Here, we have used the notations $\phi_\tau = \partial\phi/\partial\tau$, $\phi_{XX} = \partial^2\phi/\partial X^2$, and the scaled parameters $\tilde{V}_{\rm OSL}(X,\tau) = -\tilde{V}_s\cos(4\pi X/A) - \tilde{V}_l\cos(2\pi X/A - 2v\tau/A^2)$ with $\tilde{V}_s = V_s/(2A^2)$ and $\tilde{V}_l = V_l/(2A^2)$, and $\tilde{\gamma} = \gamma/A$.

As the benchmark, we recall that without the pump ($\tilde{V}_{\rm OSL} = 0$), there exist two special cases where known solutions exist. (i) Without both the nonlinearity and the pump, Eq. (4) is reduced to the familiar linear Schrödinger equation with the δ potential, whose solution is a bound state localized in the defect potential (see, e.g., Ref. [53,54] and the references therein), i.e., $\phi_{\rm im}(X) = \sqrt{\tilde{\gamma}}e^{-\tilde{\gamma}|X|}$ with the localization length $1/\tilde{\gamma}$. (ii) Without the impurity ($\tilde{\gamma} = 0$) and the pump, Eq. (4) supports moving solitons of the form $\phi_{\rm soliton} = \eta{\rm sech}[\eta(X - \kappa\tau)]\exp[i(\eta^2 - \kappa^2)\tau/2 + i\kappa X]$ [53], with the amplitude η, width $1/\eta$, and momentum κ. In the presence of the Thouless pump [$\tilde{V}_{\rm OSL}(X,\tau) \neq 0$], neither the bound state $\phi_{\rm im}$ nor the soliton $\phi_{\rm soliton}$ stands as the general solutions of Eq. (4). To seek the solutions in this case, we use the Lagrangian variational approach along the line of Refs. [53,54]. We assume a trial wave function, which is the combination of the moving soliton and the impurity-induced bound state, i.e.,

$$\phi(X,\tau) = [\eta{\rm sech}(\eta X - z)e^{i\kappa X} + a\sqrt{\tilde{\gamma}}e^{-\tilde{\gamma}|X|+i\alpha}]e^{i\beta}, \quad (5)$$

where $\eta(\tau)$, $z(\tau)$, $\kappa(\tau)$, $a(\tau)$, $\alpha(\tau)$, and $\beta(\tau)$ are the variational parameters to be determined below. Specifically, $\eta(\tau)$ and $z(\tau)$ are the amplitude and the center-of-mass position of the soliton, respectively, $\kappa(\tau)$ is the wave number of the soliton, $a(\tau)$ is the amplitude of the bound-state component, $\alpha(\tau)$ is the relative phase between the soliton and the bound

state, and $\beta(\tau)$ is the global phase of the trial function. The key assumption underlying the ansatz (5) is that the functional forms of the soliton and the impurity-induced bound state are preserved in the presence of the Thouless pumping, but the corresponding parameters become slowly time dependent.

With Eq. (5), the Lagrangian of L corresponding to the GP Eq. (4) can be derived following standard procedures [53,54]. The Lagrangian is written as

$$L = \frac{i}{2}\int_{-\infty}^{+\infty}\left(\phi^{\star}\frac{\partial\phi}{\partial\tau} - \phi\frac{\partial\phi^{\star}}{\partial\tau}\right)dX - E, \tag{6}$$

where we have

$$\begin{aligned} E = {} & \frac{1}{2}\int_{-\infty}^{+\infty}\left|\frac{\partial\phi}{\partial X}\right|^2 dX - \frac{1}{2}\int_{-\infty}^{+\infty}|\phi|^4 dX \\ & - \int_{-\infty}^{+\infty}\tilde{\gamma}\delta(X)|\phi|^2 dX - \int_{-\infty}^{+\infty}\tilde{V}_s\cos\left(\frac{4\pi X}{A}\right)|\phi|^2 dX \\ & - \int_{-\infty}^{+\infty}\tilde{V}_l\cos\left(\frac{2\pi X}{A} - \frac{2\nu\tau}{A^2}\right)|\phi|^2 dX. \end{aligned}$$

Inserting ansatz (5) into Eq. (6), and after some tedious calculations as detailed in Appendix C, the Lagrangian is derived as

$$\begin{aligned} L = {} & -2\eta\frac{\partial\beta}{d\tau} - 2z\frac{\partial\kappa}{\partial\tau} - \kappa^2\eta + \frac{1}{3}\eta^3 + 2\pi^2\left[\frac{2\tilde{V}_s}{A}\cos\left(\frac{4\pi z}{\eta A}\right)\mathrm{csch}\left(\frac{2\pi^2}{\eta A}\right) + \frac{\tilde{V}_l}{A}\cos\left(\frac{2\pi A z - 2\eta\nu\tau}{\eta A^2}\right)\mathrm{csch}\left(\frac{\pi^2}{\eta A}\right)\right] \\ & + \tilde{\gamma}\eta^2\mathrm{sech}^2(z) + 2(a\tilde{\gamma}^{3/2})\eta\mathrm{sech}(z)\cos(\alpha) - a^2\left(\frac{\partial\beta}{\partial\tau} + \frac{\partial\alpha}{\partial\tau}\right) + \frac{a^2\tilde{\gamma}^2}{2} + \frac{a^2\tilde{\gamma}^2A^2\tilde{V}_s}{4\pi^2 + A^2\tilde{\gamma}^2} + \frac{a^2\tilde{\gamma}^2A^2\tilde{V}_l}{\pi^2 + A^2\tilde{\gamma}^2}\cos\left(\frac{2\nu\tau}{A^2}\right) + \frac{1}{4}a^4\tilde{\gamma}. \end{aligned} \tag{7}$$

The first line of Lagrangian (7) does not depend on impurity parameters, corresponding to the contribution from the pumped soliton in the absence of impurity. The second line involves the corrections due to impurities up to the fourth orders of a associated with the weight of bound-state component in Eq. (5) [53]. In particular, the terms in order of $O(a^1)$ come from the mutual interaction between the bound state and the soliton; the terms in order of $O(a^2)$ describe the impurity's energy in the presence of the pumping potential; the terms in order of $O(a^4)$ arise from the self-interaction of the bound state.

Thus the Euler-Lagrange equations for the variational parameters are given by $\frac{\partial L}{\partial q_i} - \frac{d}{d\tau}(\frac{\partial L}{\partial \dot{q}_i}) = 0$ with $q_i = \eta, z, \kappa, a, \alpha, \beta$. After some tedious but straightforward calculations, we obtain Eqs. (8)–(13) below

$$\frac{d}{d\tau}z = \eta\kappa, \tag{8}$$

$$\frac{d}{d\tau}a = \eta\tilde{\gamma}^{3/2}\mathrm{sech}(z)\sin(\alpha), \tag{9}$$

$$\frac{d}{d\tau}\eta = -a\eta\tilde{\gamma}^{3/2}\mathrm{sech}(z)\sin(\alpha), \tag{10}$$

$$\begin{aligned} \frac{d}{d\tau}\kappa = {} & -\frac{8\pi^3\tilde{V}_s}{A^2\eta}\mathrm{csch}\left(\frac{2\pi^2}{A\eta}\right)\sin\left(\frac{4\pi z}{A\eta}\right) - \frac{2\pi^3\tilde{V}_l}{A^2\eta}\mathrm{csch}\left(\frac{\pi^2}{A\eta}\right)\sin\left(\frac{2A\pi z - 2\nu\tau\eta}{A^2\eta}\right) - \tilde{\gamma}\eta^2\mathrm{sech}^2(z)\tanh(z) \\ & - a\eta\tilde{\gamma}^{3/2}\cos(\alpha)\mathrm{sech}(z)\tanh(z), \end{aligned} \tag{11}$$

$$\frac{d}{d\tau}\alpha = \frac{1}{a}\cos(\alpha)\mathrm{sech}(z)\eta\tilde{\gamma}^{3/2} + \frac{1}{2}a^2\tilde{\gamma} - \frac{d}{d\tau}\beta + \frac{\tilde{\gamma}^2}{2} + \frac{A^2\tilde{V}_l\tilde{\gamma}^2}{\pi^2 + A^2\tilde{\gamma}^2}\cos\left(\frac{2\nu\tau}{A^2}\right) + \frac{A^2\tilde{V}_s\tilde{\gamma}^2}{4\pi^2 + A^2\tilde{\gamma}^2}, \tag{12}$$

$$\begin{aligned} \frac{d}{d\tau}\beta = {} & \frac{4\pi^4\tilde{V}_s}{A^2\eta^2}\cos\left(\frac{4\pi z}{A\eta}\right)\coth\left(\frac{2\pi^2}{A\eta}\right)\mathrm{csch}\left(\frac{2\pi^2}{A\eta}\right) + \frac{8\pi^3\tilde{V}_s}{A^2\eta^2}\mathrm{csch}\left(\frac{2\pi^2}{A\eta}\right)\sin\left(\frac{4\pi z}{A\eta}\right)z \\ & + \frac{\pi^4\tilde{V}_l}{A^2\eta^2}\cos\left(\frac{2A\pi z - 2\tau\nu\eta}{A^2\eta}\right)\coth\left(\frac{\pi^2}{A\eta}\right)\mathrm{csch}\left(\frac{\pi^2}{A\eta}\right) + \frac{2\pi^3\tilde{V}_l}{A^2\eta^2}\mathrm{csch}\left(\frac{\pi^2}{A\eta}\right)\sin\left(\frac{2A\pi z - 2\tau\nu\eta}{A^2\eta}\right)z \\ & + \tilde{\gamma}\mathrm{sech}^2(z)\eta + \frac{1}{2}\eta^2 - \frac{\kappa^2}{2} + a\tilde{\gamma}^{3/2}\cos(\alpha)\mathrm{sech}(z). \end{aligned} \tag{13}$$

Equation (8), along with Eqs. (9)–(13), provides the key analytical result of this work; it shows how the motion of a soliton against an impurity is affected by the Thouless pump. Note that without the pump (i.e., $\tilde{V}_s = \tilde{V}_l = 0$), the above equations recover the corresponding results of Ref. [53]. As shown in Eq. (8), the displacement of the soliton is strongly affected by the time-dependent superposition amplitudes of the soliton component $\eta(\tau)$ and the bound-state component $a(\tau)$ in Eq. (10).

To solve the set of Euler-Lagrange equations in Eqs. (8)–(13) for the variational parameters, without loss of generality, we consider the following initial conditions. At $\tau = 0$, the position of the bright soliton is centered at $z(0)/A = -3$, far away from the impurity; the initial amplitude and velocity of

the soliton are chosen as $\eta = 1$ and $\kappa = 0.0258$, respectively; for other parameters, we choose $a(0) = \alpha(0) = \beta(0) = 0$.

To double check whether our derivations reproduce the known results in Ref. [53] in the absence of Thouless pumps, at first, we take $\tilde{V}_s = 0$ and $\tilde{V}_l = 0$ in Eqs. (8)–(13). Indeed, as illustrated in Fig. 1(c) for the weak impurity with $\tilde{\gamma} = 0.026$, the soliton directly transits through the impurity potential without being localized. This can be intuitively understood by noting that for small $\tilde{\gamma}$, the bound state has a much smaller energy than the soliton, resulting in a small admixture of the localized bound state in Eq. (5). Therefore, the moving soliton is only slightly perturbed by the impurity. With the increase of $\tilde{\gamma}$, however, the bound state gains more weight in the wave function described by Eq. (5). For $\tilde{\gamma} = 0.137$ as in Fig. 2(c), we see that the initially moving soliton becomes localized around the impurity, consistent with previous findings.

Next, we turn on the Thouless pump with $\tilde{V}_s = \tilde{V}_l = 0.83$ (corresponding to $V_s = V_l = 25$ and $A^2 = 15$), and again solve Eqs. (8)–(13). The result for the weak impurity is shown in Fig. 1(d). We see that the soliton in the Thouless pump passes through a weak impurity as if the impurity does not exist, and its mean displacement in a period becomes quantized. Remarkably, as shown in Fig. 2(d), the nonlinear topological pump enables the soliton to pass through even for strong impurity strength, contrary to the pump-free case, and the motion is quantized. This provides a direct evidence that the quantized transport of a quantum particle in nonlinear topological Thouless pump is robust against the local imperfections.

V. DISCUSSION

In previous sections, we have illustrated the robustness of the nonlinear Thouless pumping of solitons against an δ impurity when $A^2 = 15$ and $V_s = V_l = 25$. In this section, we extend our discussions to general conditions of the impurity, the soliton, and the lattice, respectively.

As mentioned earlier, numerically, the δ impurity is approximated by a narrow Gaussian function $-\gamma\delta(x) = -\lim_{\sigma\to 0} \frac{\gamma}{\sqrt{2\pi}\sigma} e^{-x^2/(2\sigma^2)}$. For instance, in Fig. 2(b) with $\gamma = 0.53$, a sufficiently small impurity width $\sigma = 0.002$ was chosen, so that without both the pump and nonlinearity the numerical solution of the system's ground state agrees perfectly with the exact solution of the bound state $\sqrt{\gamma}e^{-\gamma|x|}$. In this limit, we see that the soliton, arrested by the impurity in free space, can undergo a quantized transport through the impurity. Increasing σ away from the δ-function limit, as in a more realistic defect with finite width, the soliton in free space remains trappable by the impurity with the width $\sigma \ll l$ smaller than the soliton width l, as shown in Fig. 3(a) for $\sigma = 0.02$ and $l = 0.4$. However, for $\sigma \gtrsim l$, the soliton can transmit through the impurity even without the pump [Fig. 3(c)]. In both cases, adding Thouless pump results in topologically quantized soliton motion through the impurity [Figs. 3(b) and 3(d)]; the average displacement is quantized to the Chern number of the lowest band.

Changing the lattice strength V_s and V_l results in modifications of the underlying band structures. Figure 4(a) considers a decreased lattice strength, $V_s = V_l = 10$, while other parameters are the same as in Fig. 2(b). Although the energy gap becomes smaller, the topology of the relevant bands remains

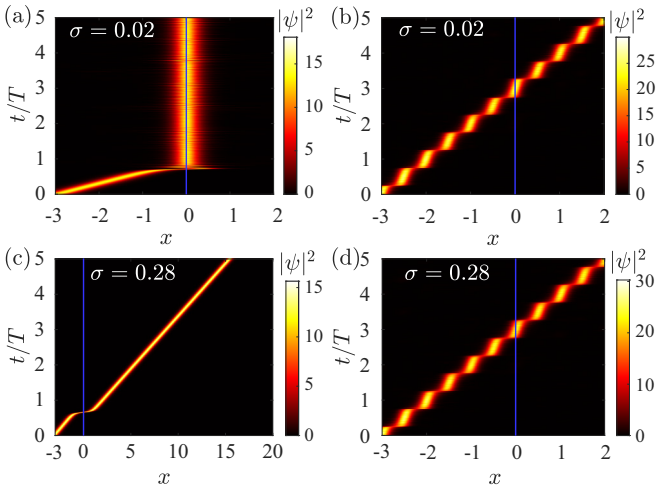

FIG. 3. Numerical simulations of soliton transport in the presence of a Gaussian impurity $-\frac{\gamma}{\sqrt{2\pi}\sigma} e^{-x^2/(2\sigma^2)}$ with $\gamma = 0.53$, for the finite width $\sigma = 0.02$ in (a) and (b), and $\sigma = 0.28$ in (c) and (d). Numerical computations are performed based on the GP Eq. (2), in free space ($V_s = V_l = 0$) in (a) and (c), and with Thouless pump ($V_s = V_l = 25$) in (b) and (d). Other parameters are the same as Fig. 2(b).

the same as for $V_s = V_l = 25$. Thus, the soliton is expected to display similar behavior as in Fig. 2(b), as seen in Fig. 4(c). Figure 4(b) shows the band structure associated with the linear pump with $V_s = 25$ and $V_l = 50$, where the Chern number of the lowest band remains to be $C = 1$, but the Chern number of the second band is different from Fig. 4(a). Since the given soliton mainly occupies the lowest band, still, similar topological soliton transmission across the impurity is observed [Fig. 4(d)], where the average displacement is predicted by the Chern number $C = 1$ of the lowest band.

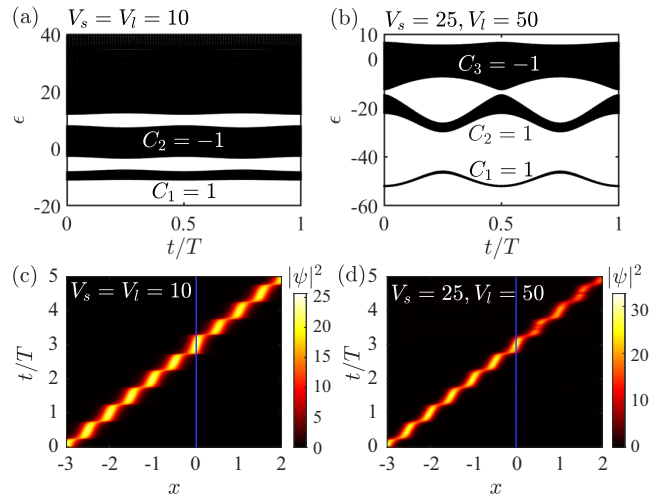

FIG. 4. Numerical simulations of soliton transport in the presence of strong impurity potential, for Thouless pump with $V_s = V_l = 10$ in (a) and (c), and $V_s = 25$ and $V_l = 50$ in (b) and (d). (a) and (b) show the corresponding band structures associated with the linear pump. The lowest two bands have Chern numbers (a) $C = \{1, -1\}$, and (b) $C = \{1, 1\}$. (c) and (d) show the corresponding soliton motion. Other parameters are same as Fig. 2(b).

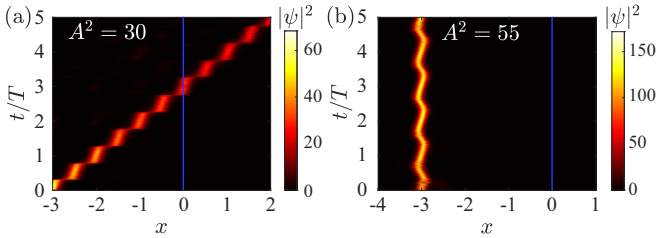

FIG. 5. Numerical simulations of soliton transport for strong impurity strength when (a) $A^2 = 30$ and (b) $A^2 = 55$. Other parameters are the same as in Fig. 2(b).

The topological transmission through the impurity is generally observed when the strength of the nonlinearity is in the pumped regime [Fig. 5(a)]. For sufficiently strong nonlinearity above the critical value, the soliton becomes to be trapped near its initial position away from the impurity, as shown in Fig. 5(b). Overall, our above results suggest that, as same as the linear case, the nonlinear topological pump is immune to microscopic imperfections.

VI. CONCLUSION

In this work, we theoretically investigate the nonlinear Thouless pumping of a soliton in the presence of an impurity based on the system of a quasi-1D BEC. Using both the GP equation and the Lagrangian variational method, we compare the interaction between the impurity and the soliton in the absence and presence of the nonlinear topological pumps. Without the pump, whether the soliton can move through the impurity depends crucially on the impurity mass. In contrast, the soliton in the nonlinear Thouless pump can transmit through even for strong impurity strength and exhibits a quantized motion. This work sheds light on the interplay of nonlinearity, topology, and disorder, and promises potential applications in information processing with solitons.

ACKNOWLEDGMENTS

We thank Qidong Fu, Fangwei Ye, Qi Zhang, and Biao Wu for stimulating discussions. This work was supported by the National Natural Science Foundation of China (Grants No. 12074344, No. 12374246), the Zhejiang Provincial Natural Science Foundation (Grant No. LZ21A040001), and the key projects of the Natural Science Foundation of China (Grant No. 11835011). Y.H. acknowledges support by Beijing National Laboratory for Condensed Matter Physics (Grant No. 2023BNLCMPKF001).

APPENDIX A: NUMERICAL METHOD

We numerically solve the dimensionless GP Eq. (2) of the main text by the split-step fast Fourier algorithm (see, e.g., Ref. [59] and the references therein). In this section, we present details on our numerical techniques.

By approximating $-\gamma\delta(x) = -\frac{\gamma}{\sqrt{2\pi}\sigma}e^{-x^2/(2\sigma^2)}$, we rewrite Eq. (2) of the main text as

$$i\frac{\partial\psi}{\partial t} = (O_1 + O_2)\psi, \tag{A1}$$

where the two operators are

$$O_1 = -\frac{1}{2}\frac{\partial^2}{\partial x^2},$$
$$O_2 = V_{\mathrm{OSL}}(x,t) - |\psi|^2 - \frac{\gamma}{\sqrt{2\pi}\sigma}e^{-x^2/(2\sigma^2)}.$$

We have $[O_1, O_2] \neq 0$. To solve the time evolution, we implement the first-order splitting scheme

$$\psi(x, t+dt) = \exp(-iO_1 dt)\exp(-iO_2 dt)\psi(x,t) \tag{A2}$$

with a sufficiently small time step $dt = 10^{-4}$. We use the fast Fourier transform (FFT) algorithm to compute Eq. (A2): let $\mathcal{F}$ denote the Fourier transform and $\mathcal{F}^{-1}$ denote the inverse Fourier transform, we have

$$\psi(x, t+dt) = \mathcal{F}^{-1}\left[\exp\left(-\frac{i}{2}k^2 dt\right)\mathcal{F}[\exp(-iO_2 dt)\psi(x,t)]\right]. \tag{A3}$$

Finally, we choose $dx = 5 \times 10^{-4}$ in the spatial discretization of the GP equation.

Using the above numerical scheme, we have reproduced the known results of soliton motion for $\gamma = 0$ in the absence of impurity, as well as the exact solutions of the bound state when both the nonlinearity and the pump are absent. In the presence of both the pump and the impurity, our numerical simulations of the soliton motion find good agreement with the results obtained from the variational approach.

APPENDIX B: CHERN NUMBER

In this section, we follow the standard procedures to calculate Chern numbers of the bands underlying the linear Thouless pump (see, e.g., Ref. [4]). The adiabatic motion of a quantum particle moving in a slowly varying periodic potential is described by the Schrödinger equation ($\hbar \equiv 1$)

$$i\frac{\partial}{\partial t}\psi = -\frac{1}{2}\frac{\partial^2}{\partial x^2}\psi + V_{\mathrm{OSL}}(x,t)\psi, \tag{B1}$$

where the dimensionless Hamiltonian reads as

$$H = -\frac{1}{2}\frac{\partial^2}{\partial x^2} - V_{\mathrm{s}}\cos^2\left(\frac{2\pi x}{d}\right) - V_{\mathrm{l}}\cos^2\left(\frac{\pi x}{d} - \nu t\right). \tag{B2}$$

Using the Bloch's theorem $\psi(x,t) = e^{-ikx}u(x,t)$ where $u(x+d,t) = u(x,t)$ and the quasimomentum $k \in \mathrm{BZ}$, we make the expansion $\psi(x,t) = e^{-ikx}\sum_{n=-\infty}^{\infty} c_n(t)e^{inQx}$, where $Q = 2\pi/d$ and $c_n(t)$ are expansion coefficients. Inserting this expansion into Eq. (B1), and denoting $\mathbf{c}(t) = (\ldots c_{-1}, c_0, c_1 \ldots)^T$, we formally obtain

$$i\frac{\partial}{\partial t}\mathbf{c} = \tilde{H}(k,t)\mathbf{c}. \tag{B3}$$

Here, the effective Hamiltonian matrix $\tilde{H}(k,t)$ has parametric dependence on time t, and satisfies $\tilde{H}(k, t+T) = \tilde{H}(k,t)$ with the time periodicity $T = \pi/\nu$.

In the numerical calculation, the expansion is usually truncated at $\pm n_{\max} = \pm M$ leading to the truncated matrix $\tilde{H}(k,t)$

with the dimension $(2M+1)\times(2M+1)$, which is written as

$$\tilde{H}(k,t)=\frac{1}{4}\begin{pmatrix} \ddots & & & & & & & \\ \cdots & h_{-2} & -V_l\xi(t) & -V_s & & & & \\ \cdots & -V_l\xi^\star(t) & h_{-1} & -V_l\xi(t) & -V_s & & & \\ & -V_s & -V_l\xi^\star(t) & h_0 & -V_l\xi(t) & -V_s & & \\ & & -V_s & -V_l\xi^\star(t) & h_1 & -V_l\xi(t) & \cdots & \\ & & & -V_s & -V_l\xi^\star(t) & h_2 & \cdots & \\ & & & & & & \ddots & \end{pmatrix}_{(2M+1)\times(2M+1)}, \tag{B4}$$

where the diagonal matrix element is $h_n=2(k-nQ)^2-2V_s-2V_l$ for $n=-M,\ldots,M$, and $\xi(t)=\exp(2i\nu t)$.

Finally, we diagonalize the truncated matrix $\tilde{H}(k,t)$ to obtain the adiabatic eigenstates $\phi_\mu(k,t)$ and corresponding eigenvalues $\epsilon_\mu(k,t)$ ($\mu=1,\ldots,2M+1$). These eigenvalues form band structures in the two-dimensional parameter space (k,t). The Chern number C_μ associated with the μth band is then defined as [4]

$$C_\mu=\frac{i}{2\pi}\int_0^T dt\int_{\mathrm{BZ}} dk[\langle\partial_t\phi_\mu|\partial_k\phi_\mu\rangle-\langle\partial_k\phi_\mu|\partial_t\phi_\mu\rangle]. \tag{B5}$$

Following the above procedures, one reproduces the known results in the case of linear topological pump (e.g., Refs. [5,27]). In our paper, $M=10$ is sufficient for calculating the Chern numbers of the band structures.

APPENDIX C: DERIVATION OF THE LAGRANGIAN

Here, we detail the derivation of the Lagrangian in Eq. (7) in the main text. Inserting ansatz (5) into Eq. (6), and after some tedious calculation, we obtain the following terms:

$$\begin{aligned} L_1&=\frac{i}{2}\int_{-\infty}^{+\infty}\left(\phi^\star\frac{\partial\phi}{\partial\tau}-\phi\frac{\partial\phi^\star}{\partial\tau}\right)dX\\ &=-(2\eta+a^2)\frac{\partial\beta}{\partial\tau}-2z\frac{\partial\kappa}{\partial\tau}-a^2\frac{\partial\alpha}{\partial\tau}. \end{aligned} \tag{C1}$$

The term associated with kinetic energy is calculated as

$$\begin{aligned} L_2&=-\frac{1}{2}\int_{-\infty}^{+\infty}\left|\frac{\partial\phi}{\partial X}\right|^2dX\\ &=-\left(\kappa^2\eta+\frac{1}{3}\eta^3+\frac{1}{2}a^2\tilde{\gamma}^2\right). \end{aligned} \tag{C2}$$

The nonlinear term is evaluated as

$$\begin{aligned} L_3&=\frac{1}{2}\int_{-\infty}^{+\infty}|\phi|^4dX\\ &=\frac{2}{3}\eta^3+\frac{1}{4}a^4\tilde{\gamma}. \end{aligned} \tag{C3}$$

The contribution from the impurity is given by

$$\begin{aligned} L_4&=\int_{-\infty}^{+\infty}\tilde{\gamma}\delta(X)|\phi|^2dX\\ &=\tilde{\gamma}[\eta^2\mathrm{sech}^2(z)+2a\eta\mathrm{sech}(z)\tilde{\gamma}^{1/2}\cos(\alpha)+a^2\tilde{\gamma}]. \end{aligned} \tag{C4}$$

The term associated with the pump reads as

$$\begin{aligned} L_5&=\int_{-\infty}^{+\infty}\left[\tilde{V}_s\cos\left(\frac{4\pi X}{A}\right)\right.\\ &\quad\left.+\tilde{V}_l\cos\left(\frac{2\pi X}{A}-\frac{2\nu\tau}{A^2}\right)\right]|\phi|^2dX\\ &=\tilde{V}_s\left[\frac{4\pi^2}{A}\cos\left(\frac{4\pi z}{A\eta}\right)\mathrm{csch}\left(\frac{2\pi^2}{A\eta}\right)+\frac{a^2\tilde{\gamma}^2A^2}{4\pi^2+A^2\tilde{\gamma}^2}\right]\\ &\quad+\frac{2\pi^2\tilde{V}_l}{A}\cos\left(\frac{2\pi Az-2\eta\nu\tau}{A^2\eta}\right)\mathrm{csch}\left(\frac{\pi^2}{A\eta}\right)\\ &\quad+\frac{a^2\tilde{\gamma}^2A^2\tilde{V}_l}{\pi^2+A^2\tilde{\gamma}^2}\cos\left(\frac{2\nu\tau}{A^2}\right). \end{aligned} \tag{C5}$$

In the above derivations, we have neglected all the terms associated with the overlapping of the two components (i.e., solitonic component and the bounded component) of the ansatz. Physically, this means that we ignore the interaction between the soliton and the impurity when they are far from each other, while retaining their interaction when the soliton is close to the impurity [53].

Finally, following from Eqs. (C1)–(C5), we arrive at Eq. (7) through the summation $L=L_1+L_2+L_3+L_4+L_5$.

[1] D. J. Thouless, M. Kohmoto, M. P. Nightingale, and M. den Nijs, Quantized Hall conductance in a two-dimensional periodic potential, Phys. Rev. Lett. **49**, 405 (1982).

[2] D. J. Thouless, Quantization of particle transport, Phys. Rev. B **27**, 6083 (1983).

[3] Q. Niu and D. J. Thouless, Quantised adiabatic charge transport in the presence of substrate disorder and many-body interaction, J. Phys. A: Math. Gen. **17**, 2453 (1984).

[4] D. Xiao, M.-C. Chang, and Q. Niu, Berry phase effects on electronic properties, Rev. Mod. Phys. **82**, 1959 (2010).

[5] L. Wang, M. Troyer, and X. Dai, Topological charge pumping in a one-dimensional optical lattice, Phys. Rev. Lett. **111**, 026802 (2013).

[6] M. Lohse, C. Schweizer, O. Zilberberg, M. Aidelsburger, and I. Bloch, A thouless quantum pump with ultracold bosonic atoms in an optical superlattice, Nature Phys. **12**, 350 (2016).

[7] S. Nakajima, T. Tomita, S. Taie, T. Ichinose, H. Ozawa, L. Wang, M. Troyer, and Y. Takahashi, Topological thouless pumping of ultracold fermions, Nature Phys. **12**, 296 (2016).

[8] H.-I. Lu, M. Schemmer, L. M. Aycock, D. Genkina, S. Sugawa, and I. B. Spielman, Geometrical pumping with a Bose-Einstein condensate, Phys. Rev. Lett. **116**, 200402 (2016).

[9] M. Lohse, C. Schweizer, H. M. Price, O. Zilberberg, and I. Bloch, Exploring 4D quantum Hall physics with a 2D topological charge pump, Nature (London) **553**, 55 (2018).

[10] S. Nakajima, N. Takei, K. Sakuma, Y. Kuno, P. Marra, and Y. Takahashi, Competition and interplay between topology and quasi-periodic disorder in Thouless pumping of ultracold atoms, Nature Phys. **17**, 844 (2021).

[11] J. Minguzzi, Z. Zhu, K. Sandholzer, A.-S. Walter, K. Viebahn, and T. Esslinger, Topological pumping in a floquet-bloch band, Phys. Rev. Lett. **129**, 053201 (2022).

[12] Y. E. Kraus, Y. Lahini, Z. Ringel, M. Verbin, and O. Zilberberg, Topological states and adiabatic pumping in quasicrystals, Phys. Rev. Lett. **109**, 106402 (2012).

[13] Y. Ke, X. Qin, F. Mei, H. Zhong, Y. S. Kivshar, and C. Lee, Topological phase transitions and Thouless pumping of light in photonic waveguide arrays, Laser Photon. Rev. **10**, 995 (2016).

[14] O. Zilberberg, S. Huang, J. Guglielmon, M. Wang, K. P. Chen, Y. E. Kraus, and M. C. Rechtsman, Photonic topological boundary pumping as a probe of 4D quantum Hall physics, Nature (London) **553**, 59 (2018).

[15] A. Cerjan, M. Wang, S. Huang, K. P. Chen, and M. C. Rechtsman, Thouless pumping in disordered photonic systems, Light Sci. Appl. **9**, 178 (2020).

[16] P. Wang, Q. Fu, R. Peng, Y. V. Kartashov, L. Torner, V. V. Konotop, and F. Ye, Two-dimensional Thouless pumping of light in photonic moiré lattices, Nature Commun. **13**, 6738 (2022).

[17] W. Ma, L. Zhou, Q. Zhang, M. Li, C. Cheng, J. Geng, X. Rong, F. Shi, J. Gong, and J. Du, Experimental observation of a generalized thouless pump with a single spin, Phys. Rev. Lett. **120**, 120501 (2018).

[18] V. M. Bastidas, Topological Thouless pumping in arrays of coupled spin chains, Phys. Rev. B **106**, L220308 (2022).

[19] D. Leykam and Y. D. Chong, Edge solitons in nonlinear-photonic topological insulators, Phys. Rev. Lett. **117**, 143901 (2016).

[20] J. Tangpanitanon, V. M. Bastidas, S. Al-Assam, P. Roushan, D. Jaksch, and D. G. Angelakis, Topological pumping of photons in nonlinear resonator arrays, Phys. Rev. Lett. **117**, 213603 (2016).

[21] A. Bisianov, M. Wimmer, U. Peschel, and O. A. Egorov, Stability of topologically protected edge states in nonlinear fiber loops, Phys. Rev. A **100**, 063830 (2019).

[22] S. K. Ivanov, Y. V. Kartashov, A. Szameit, L. Torner, and V. V. Konotop, Vector topological edge solitons in floquet insulators, ACS Photon. **7**, 735 (2020).

[23] T. Dai, Y. Ao, J. Mao, Y. Yang, Y. Zheng, C. Zhai, Y. Li, J. Yuan, B. Tang, Z. Li, J. Luo, W. Wang, X. Hu, Q. Gong, and J. Wang, Non-Hermitian topological phase transitions controlled by nonlinearity, Nature Phys. **20**, 101 (2024).

[24] D. D. Solnyshkov, O. Bleu, B. Teklu, and G. Malpuech, Chirality of topological gap solitons in bosonic dimer chains, Phys. Rev. Lett. **118**, 023901 (2017).

[25] D. González-Cuadra, A. Dauphin, P. R. Grzybowski, M. Lewenstein, and A. Bermudez, Dynamical solitons and boson fractionalization in cold-atom topological insulators, Phys. Rev. Lett. **125**, 265301 (2020).

[26] P.-W. Lo, C. D. Santangelo, B. G.-g. Chen, C.-M. Jian, K. Roychowdhury, and M. J. Lawler, Topology in nonlinear mechanical systems, Phys. Rev. Lett. **127**, 076802 (2021).

[27] M. Jürgensen, S. Mukherjee, and M. C. Rechtsman, Quantized nonlinear thouless pumping, Nature (London) **596**, 63 (2021).

[28] N. Mostaan, F. Grusdt, and N. Goldman, Quantized topological pumping of solitons in nonlinear photonics and ultracold atomic mixtures, Nature Commun. **13**, 5997 (2022).

[29] Q. Fu, P. Wang, Y. V. Kartashov, V. V. Konotop, and F. Ye, Nonlinear thouless pumping: solitons and transport breakdown, Phys. Rev. Lett. **128**, 154101 (2022).

[30] Q. Fu, P. Wang, Y. V. Kartashov, V. V. Konotop, and F. Ye, Two-dimensional nonlinear thouless pumping of matter waves, Phys. Rev. Lett. **129**, 183901 (2022).

[31] M. Jürgensen and M. C. Rechtsman, Chern number governs soliton motion in nonlinear thouless pumps, Phys. Rev. Lett. **128**, 113901 (2022).

[32] M. Jürgensen, S. Mukherjee, C. Jörg, and M. C. Rechtsman, Quantized fractional Thouless pumping of solitons, Nature Phys. **19**, 420 (2023).

[33] T. Tuloup, R. W. Bomantara, and J. Gong, Breakdown of quantization in nonlinear Thouless pumping, New J. Phys. **25**, 083048 (2023).

[34] R. Citro and M. Aidelsburger, Thouless pumping and topology, Nature Rev. Phys. **5**, 87 (2023).

[35] Z.-C. Xiang, K. Huang, Y.-R. Zhang *et al.*, Simulating Chern insulators on a superconducting quantum processor, Nature Commun. **14**, 5433 (2023).

[36] E. Berg, M. Levin, and E. Altman, Quantized pumping and topology of the phase diagram for a system of interacting bosons, Phys. Rev. Lett. **106**, 110405 (2011).

[37] Y. Qian, M. Gong, and C. Zhang, Quantum transport of bosonic cold atoms in double-well optical lattices, Phys. Rev. A **84**, 013608 (2011).

[38] F. Grusdt and M. Höning, Realization of fractional Chern insulators in the thin-torus limit with ultracold bosons, Phys. Rev. A **90**, 053623 (2014).

[39] T.-S. Zeng, W. Zhu, and D. N. Sheng, Fractional charge pumping of interacting bosons in one-dimensional superlattice, Phys. Rev. B **94**, 235139 (2016).

[40] R. Li and M. Fleischhauer, Finite-size corrections to quantized particle transport in topological charge pumps, Phys. Rev. B **96**, 085444 (2017).

[41] Y. Ke, X. Qin, Y. S. Kivshar, and C. Lee, Multiparticle Wannier states and Thouless pumping of interacting bosons, Phys. Rev. A **95**, 063630 (2017).

[42] L. Taddia, E. Cornfeld, D. Rossini, L. Mazza, E. Sela, and R. Fazio, Topological fractional pumping with alkaline-earth-like atoms in synthetic lattices, Phys. Rev. Lett. **118**, 230402 (2017).

[43] A. Hayward, C. Schweizer, M. Lohse, M. Aidelsburger, and F. Heidrich-Meisner, Topological charge pumping in the interacting bosonic Rice-Mele model, Phys. Rev. B **98**, 245148 (2018).

[44] M. Nakagawa, T. Yoshida, R. Peters, and N. Kawakami, Breakdown of topological Thouless pumping in the strongly interacting regime, Phys. Rev. B **98**, 115147 (2018).

[45] L. Stenzel, A. L. C. Hayward, C. Hubig, U. Schollwöck, and F. Heidrich-Meisner, Quantum phases and topological properties of interacting fermions in one-dimensional superlattices, Phys. Rev. A **99**, 053614 (2019).

[46] T. Haug, R. Dumke, L.-C. Kwek, and L. Amico, Topological pumping in Aharonov-Bohm rings, Commun. Phys. **2**, 127 (2019).

[47] R. Unanyan, M. Kiefer-Emmanouilidis, and M. Fleischhauer, Finite-temperature topological invariant for interacting systems, Phys. Rev. Lett. **125**, 215701 (2020).

[48] S. Greschner, S. Mondal, and T. Mishra, Topological charge pumping of bound bosonic pairs, Phys. Rev. A **101**, 053630 (2020).

[49] Y.-L. Chen, G.-Q. Zhang, D.-W. Zhang, and S.-L. Zhu, Simulating bosonic Chern insulators in one-dimensional optical superlattices, Phys. Rev. A **101**, 013627 (2020).

[50] V. M. Pérez-García, H. Michinel, J. I. Cirac, M. Lewenstein, and P. Zoller, Low energy excitations of a Bose-Einstein condensate: a time-dependent variational analysis, Phys. Rev. Lett. **77**, 5320 (1996).

[51] F. Dalfovo, S. Giorgini, L. P. Pitaevskii, and S. Stringari, Theory of Bose-Einstein condensation in trapped gases, Rev. Mod. Phys. **71**, 463 (1999).

[52] U. Al Khawaja, H. T. C. Stoof, R. G. Hulet, K. E. Strecker, and G. B. Partridge, Bright soliton trains of trapped Bose-Einstein condensates, Phys. Rev. Lett. **89**, 200404 (2002).

[53] K. Forinash, M. Peyrard, and B. Malomed, Interaction of discrete breathers with impurity modes, Phys. Rev. E **49**, 3400 (1994).

[54] C. Jia and Z. Liang, Interaction between an impurity and nonlinear excitations in a polariton condensate, Entropy **24**, 1789 (2022).

[55] L. Fallani, J. E. Lye, V. Guarrera, C. Fort, and M. Inguscio, Ultracold atoms in a disordered crystal of light: towards a bose glass, Phys. Rev. Lett. **98**, 130404 (2007).

[56] L. Chomaz, I. Ferrier-Barbut, F. Ferlaino, B. Laburthe-Tolra, B. L. Lev, and T. Pfau, Dipolar physics: a review of experiments with magnetic quantum gases, Rep. Prog. Phys. **86**, 026401 (2023).

[57] M. Łącki, M. A. Baranov, H. Pichler, and P. Zoller, Nanoscale "dark state" optical potentials for cold atoms, Phys. Rev. Lett. **117**, 233001 (2016).

[58] Y. Wang, S. Subhankar, P. Bienias, M. Łącki, T.-C. Tsui, M. A. Baranov, A. V. Gorshkov, P. Zoller, J. V. Porto, and S. L. Rolston, Dark state optical lattice with a subwavelength spatial structure, Phys. Rev. Lett. **120**, 083601 (2018).

[59] G. M. Muslu and H. A. Erbay, Higher-order split-step Fourier schemes for the generalized nonlinear Schrödinger equation, Math. Comput. Simulat. **67**, 581 (2005).